

## Amine–Amide Equilibrium in Gold(III) Complexes and a Gold(III)–Gold(I) Auropilic Bond

Lingyun Cao, Michael C. Jennings, and Richard J. Puddephatt\*

Department of Chemistry, University of Western Ontario, London, Canada N6A 5B7

Received October 6, 2006

The ligands  $\text{HN}(\text{CH}_2-2\text{-C}_5\text{H}_4\text{N})_2$ , BPMA, and  $\text{PhCH}_2\text{N}(\text{CH}_2-2\text{-C}_5\text{H}_4\text{N})_2$ , BBPMA, react with  $\text{Na}[\text{AuCl}_4]$  to give the cationic complexes  $[\text{AuCl}(\text{BPMA-H})]^+$  and  $[\text{AuCl}(\text{BBPMA})]^{2+}$ , respectively. The amido complex  $[\text{AuCl}(\text{BPMA-H})]^+$  undergoes easy inversion at the amido nitrogen atom and can be reversibly protonated by triflic acid to give  $[\text{AuCl}(\text{BPMA})]^{2+}$ . The complex  $[\text{AuCl}(\text{BBPMA})]^{2+}$  is easily decomposed in aqueous solution by cleavage of a carbon–nitrogen bond or, in dilute HCl solution, by protonation of the ligand to give  $[\text{BBPMAH}_2]\text{Cl}[\text{AuCl}_4]$ . The complexes  $[\text{BBPMAH}_2]\text{Cl}[\text{AuCl}_4]$  and  $[\text{BBPMAH}_2]\text{Cl}[\text{AuCl}_2]$  can be formed by direct reaction of BBPMA with  $\text{H}[\text{AuCl}_4]$ . Unusual forms of gold(III)···gold(III) and gold(III)···gold(I) auropilic bonding are observed in the salts  $[\text{AuCl}(\text{BPMA-H})]^- [\text{PF}_6]$  and  $[\text{AuCl}(\text{BPMA-H})][\text{AuCl}_2]$ , respectively. The first comparison of the structures of gold(III) amine and amido complexes, in the cations  $[\text{AuCl}(\text{BPMA-H})]^+$  and  $[\text{AuCl}(\text{BPMA})]^{2+}$ , indicates that there is little  $p_\pi\text{--}d_\pi$  bonding in the amido–gold bond and that the amide exerts a stronger trans influence than the amine group.

## Introduction

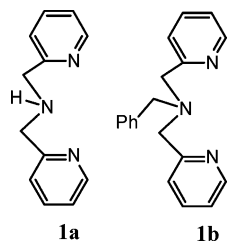
The realization that gold(I) and gold(III) complexes can have high activity in either homogeneous or heterogeneous catalysis has created a critical need for a better understanding of the role of supporting ligands for these metal ions.<sup>1</sup> In particular, ligands are needed that can prevent easy decomposition to gold metal while maintaining high catalytic activity and that can facilitate mechanistic studies of the catalytic reactions. For gold(III) catalysts, these supporting ligands should also stabilize the higher oxidation state, thus ruling out soft donor ligands such as tertiary phosphines that tend to favor gold(I).<sup>2</sup> On the other hand, many simple nitrogen-donor ligands, while effective in stabilizing gold(III) with respect to gold(I), are easily displaced from gold-

(III), in which case decomposition to metallic gold tends to occur.<sup>2</sup> One potentially useful feature of primary and secondary amine complexes of gold(III) is that the high charge on gold(III) polarizes the NH group of the coordinated amine and leads to easy deprotonation to form amido complexes.<sup>2–7</sup> These amido complexes have been known for many years,<sup>3</sup> and the effects of the deprotonation on spectroscopic properties, on the rates and mechanisms of ligand-substitution reactions, and on bioinorganic chemistry have been well established.<sup>2–8</sup> Judging from known amine–

\* Corresponding author. E-mail: pudd@uwo.ca.

- (1) (a) Hashmi, A. S. K. *Gold Bull.* **2004**, 37, 51. (b) Ivanova, S.; Petit, C.; Pitchon, V. *Gold Bull.* **2006**, 39, 3. (c) Fan, D.; Melendez, E.; Ranford, J. D.; Lee, P. F.; Vittal, J. J. *J. Organomet. Chem.* **2004**, 689, 2969. (d) Fierro-Gonzalez, J. C.; Gates, B. C. *J. Phys. Chem. B* **2004**, 108, 16999. (e) Jones, C. J.; Taube, D.; Ziatdinov, V. R.; Periana, R. A.; Nielsen, R. J.; Oxgaard, J.; Goddard, W. A. *Angew. Chem., Int. Ed.* **2004**, 43, 4626. (f) Gonzalez-Arellano, C.; Corma, A.; Iglesias, M.; Sanchez, F. *Chem. Commun.* **2005**, 3431. (g) Lo, V. K.-Y.; Liu, Y.; Wong, M.-K.; Che, C.-M. *Org. Lett.* **2006**, 8, 1529. (h) Comas-Vives, A.; Gonzalez-Arellano, C.; Corma, A.; Iglesias, M.; Sanchez, F.; Ujaque, G. *J. Am. Chem. Soc.* **2006**, 128, 4756. (i) Hashmi, A. S. K.; Bianco, M. C.; Fischer, D.; Bats, J. W. *Eur. J. Org. Chem.* **2006**, 1387.
- (2) (a) Schmidbaur, H. *Gold: Progress in Chemistry, Biochemistry and Technology*; Wiley: Chichester, U.K., 1999. (b) Puddephatt, R. J. *The Chemistry of Gold*; Elsevier: Amsterdam, 1978.
- (3) Kharasch, M. S.; Isbell, H. S. *J. Am. Chem. Soc.* **1931**, 53, 3059.
- (4) (a) Baddley, W. H.; Basolo, F.; Gray, H. B.; Nolting, C.; Poe, A. J. *Inorg. Chem.* **1963**, 2, 921. (b) Weick, C. F.; Basolo, F. *Inorg. Chem.* **1964**, 31, 576. (c) Baddley, W. H.; Basolo, F. *J. Am. Chem. Soc.* **1966**, 88, 2944.
- (5) (a) Cinellu, M. A.; Minghetti, G.; Pinna, M. V.; Stoccoro, S.; Zucca, A.; Manassero, M. *Eur. J. Inorg. Chem.* **2003**, 2304. (b) Oyaizu, K.; Ohtani, Y.; Shiozawa, A.; Sugawara, K.; Saito, T.; Yuasa, M. *Inorg. Chem.* **2005**, 44, 6915. (c) Cheung, T.-C.; Lai, T.-F.; Che, C.-M. *Polyhedron* **1994**, 13, 2073. (d) Simonov, Y.; Bologna, O.; Bourosh, P.; Gerbeleu, N.; Lipkowski, J.; Gdaniec, M. *Inorg. Chim. Acta* **2006**, 359, 2006.
- (6) (a) Cornejo, A. A.; Castineiras, A.; Yanovsky, A. I.; Nolan, K. B. *Inorg. Chim. Acta* **2003**, 349, 91. (b) Best, S. L.; Chattopadhyay, T. K.; Djuran, M. I.; Palmer, R. A.; Sadler, P. J.; Sovago, I.; Varnagy, K. *J. Chem. Soc., Dalton Trans.* **1997**, 2587. (c) Koch, D.; Sunkel, K.; Beck, W. *Z. Naturforsch. B* **1999**, 54, 96. (d) Horvath, U. E. I.; Cronje, S.; McKenzie, J. M.; Barbour, L. J.; Raubenheimer, H. G. *Z. Naturforsch. B* **2004**, 59, 1605.
- (7) (a) Bunge, S. D.; Just, O.; Rees, W. S. *Angew. Chem., Int. Ed.* **2000**, 39, 3082. (b) Burgos, M.; Crespo, O.; Gimeno, M. C.; Jones, P. G.; Laguna, A. *Eur. J. Inorg. Chem.* **2003**, 2170.

Chart 1



amide ligand properties, gold chemistry has potential in reactions such as outer-sphere hydrogenation of unsaturated groups (ketones, imines, etc.) or C–H bond activation.<sup>1,9</sup> However, to date, no structural comparisons of amine and amido complexes of gold(III) have been conducted that might provide insight into the bond-activation processes.

This article reports the chemistry of bis(2-pyridylmethyl)-amine (BPMA, **1a**) and its N-benzyl derivative, BBPMA (**1b**), with gold(III) (Chart 1). Clearly, BPMA is capable of undergoing deprotonation to form the amide, but BBPMA is not. The reactions of BPMA with square-planar palladium(II),<sup>10</sup> platinum(II),<sup>11</sup> rhodium(I),<sup>12</sup> and iridium(I)<sup>12</sup> have been reported, but we are not aware of any similar chemistry with gold(III). The first comparison of the structures of amine and amido derivatives of gold(III) is reported herein.

## Results and Discussion

**Reactions of Ligand BBPMA, 1b.** Initial attempts to prepare gold(III) complexes by reaction of BPMA or BBPMA with  $\text{H}[\text{AuCl}_4]$  were unsuccessful and resulted only in protonation of the ligand. For example, reaction of BBPMA, **1b**, with  $\text{H}[\text{AuCl}_4]$  under mild conditions gave the mixed chloride/tetrachloroaurate(III) salt  $[\text{BBPMAH}_2]\text{Cl}[\text{AuCl}_4]$ , **2a**, and under more forcing conditions, the reaction gave the corresponding chloride/dichloroaurate(I) salt  $[\text{BBPMAH}_2]\text{Cl}[\text{AuCl}_2]$ , **2b** (Scheme 1). In both salts, the chloride ion is strongly hydrogen-bonded to the  $[\text{BBPMAH}_2]^{2+}$  ion, as illustrated in Figure 1 for complex **2b**. There appears to be a slow reduction of  $[\text{AuCl}_4]^-$  to  $[\text{AuCl}_2]^-$  in this reaction medium, with release of HCl. The released chloride is strongly bound through hydrogen bonding to the doubly protonated BBPMA ligand, and the cation  $[\text{BBPMAH}_2\cdots\text{Cl}]^+$  can crystallize with either the  $[\text{AuCl}_4]^-$  or  $[\text{AuCl}_2]^-$  ion.

In neutral solution, the ligand BBPMA (**1b**) reacted with  $\text{Na}[\text{AuCl}_4]$  to give  $[\text{AuCl}(\text{BBPMA})\text{Cl}_2]$ , **3** (Scheme 2), which

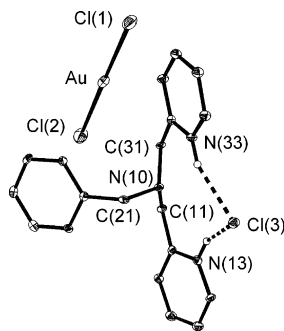
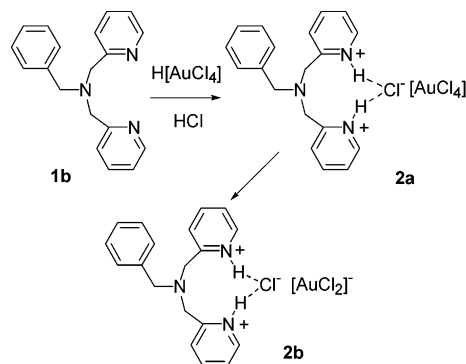
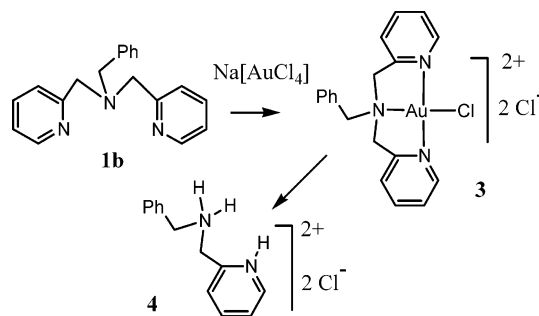


**Figure 1.** View of the structure of complex **2b**. Selected bond parameters: AuCl(1), 2.258(1); AuCl(2), 2.255(1) Å; Cl(1)AuCl(2), 179.03(5)°. Hydrogen bonding: N(13)Cl(3), 3.067(4); N(33)Cl(3), 3.061(4) Å. The structure of the tetrachloroaurate salt **2a** is similar (Figure S1).

**Scheme 1**



**Scheme 2**



was characterized by its spectroscopic properties. Most diagnostic in the  $^1\text{H}$  NMR spectrum was the observation that the methylene protons of the 2-pyridylmethyl groups of complex **3** are diastereotopic and appear as an “AB” multiplet [ $\delta(\text{H}^a) = 5.19$ ,  $\delta(\text{H}^b) = 5.87$ ,  $^2J(\text{H}^a\text{H}^b) = 14$  Hz], whereas the methylene protons of the benzyl group are equivalent and appear as a singlet resonance [ $\delta(\text{H}) = 4.85$ ]. (See Figure 2.)

Complex **3** had limited thermal stability in aqueous solution. After complete decomposition, metallic gold was

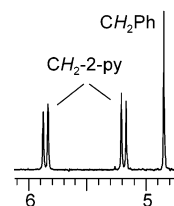
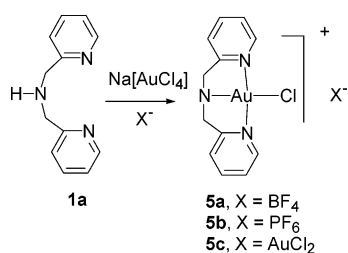


**Figure 2.** Methylene region of the  $^1\text{H}$  NMR spectrum (400 MHz,  $\text{CD}_3\text{-NO}_2$  solution) of complex **3**, showing the diastereotopic nature of the  $\text{CH}^a\text{H}^b$ –2-py protons.

- (8) Fernandez, E. J.; Gil, M.; Olmos, M. E.; Crespo, O.; Laguna, A.; Jones, P. G. *Inorg. Chem.* **2001**, *40*, 2170.
- (9) (a) Clapham, S. E.; Hadzovic, A.; Morris, R. H. *Coord. Chem. Rev.* **2004**, *248*, 2201. (b) Fulton, J. R.; Sklenak, S.; Bouwkamp, M. W.; Bergman, R. G. *J. Am. Chem. Soc.* **2002**, *124*, 4722.
- (10) (a) Bugargic, Z. D.; Liehr, G.; van Eldik, R. *J. Chem. Soc., Dalton Trans.* **2002**, 951. (b) Nagy, Z.; Fabian, I.; Benyei, A.; Sovago, I. *J. Inorg. Biochem.* **2003**, *94*, 291.
- (11) (a) Pitteri, B.; Annibale, G.; Marangoni, G.; Bertolasi, V.; Ferretti, V. *Polyhedron* **2002**, *21*, 2283. (b) Pitteri, B.; Marangoni, G.; Cattalini, L.; Visentin, F.; Bertolasi, V.; Gilli, P. *Polyhedron* **2001**, *20*, 869. (c) Jenkins, H. A.; Yap, G. P. A.; Puddephatt, R. J. *Organometallics* **1997**, *16*, 1946.
- (12) (a) Thewissen, S.; Reijnders, M. D. M.; Smits, J. M. M.; de Bruin, B. *Organometallics* **2005**, *24*, 5964. (b) de Bruin, B.; Verhagen, J. A. W.; Schouten, C. H. J.; Gal, A. W.; Feichtinger, D.; Plattner, D. A. *Chem. Eur. J.* **2001**, *7*, 416.

Scheme 3



formed, and the compound [PhCH<sub>2</sub>NHCH<sub>2</sub>–2-C<sub>5</sub>H<sub>4</sub>NH]Cl<sub>2</sub>, **4**, was isolated from the solution and characterized crystallographically (Figure S2). The formation of compound **4** involves the cleavage of a 2-C<sub>5</sub>H<sub>4</sub>NCH<sub>2</sub>–N bond of the ligand **1b** to give PhCH<sub>2</sub>NHCH<sub>2</sub>–2-C<sub>5</sub>H<sub>4</sub>N, which is then doubly protonated by HCl formed during the decomposition. The cleavage of the C–N bond is probably aided by polarization of the ligand BBPMA when bound to gold(III), and the N–CH<sub>2</sub>–2-pyridyl group is activated more than the N–CH<sub>2</sub>Ph group toward nucleophilic attack at carbon by coordination of both the amine and pyridyl units to gold(III) in complex **3**. The fate of the cleaved 2-pyridylmethyl group has not been determined. The ligand BBPMA is stable in boiling water or in dilute hydrochloric acid solution, so coordination to gold(III) is clearly involved in the ligand-cleavage reaction to give **4**.

**Reactions of the Ligand BPMA, 1a.** The gold(III) complexes [AuCl(BPMA–H)]<sup>+</sup>X<sup>–</sup>, **5a–5c**, were prepared by reaction in a neutral solution of the ligand **1a** with Na[AuCl<sub>4</sub>], as shown in Scheme 3. The reactions were usually carried out in the presence of tetrafluoroborate or hexafluorophosphate salts to give the corresponding salts **5a** (X = BF<sub>4</sub>) or **5b** (X = PF<sub>6</sub>). If no large anion was present, the cation crystallized as the dichloroaurate(I) salt **5c**. The complexes were isolated as red, light-sensitive solids. Complexes **5a** and **5b** were soluble in acetone or acetonitrile, but **5c** was sparingly soluble in most organic solvents, although it dissolved in dimethyl sulfoxide. The reactions of Scheme 3 occur with spontaneous deprotonation of the BPMA ligand to give the gold(III) amido complexes **5a–5c**.

Complexes **5** were characterized by their <sup>1</sup>H NMR spectra and by X-ray structure determinations. In complexes **5**, the NCH<sup>a</sup>H<sup>b</sup> protons are expected to be nonequivalent as a result of the trigonal-pyramidal stereochemistry at the amido nitrogen, but only a single resonance was observed for these protons in the <sup>1</sup>H NMR spectrum of each complex. For example, complex **5a** gave a resonance at δ(NCH<sub>2</sub>) = 4.42 in the <sup>1</sup>H NMR spectrum, and this peak broadened but did not split at low temperature (Figure 3).

The structure of complex **5a** is shown in Figure 4, with selected structural parameters listed in Tables 1 and 2. There are no strong interactions between the cation and the tetrafluoroborate anion, which is not shown.

In complex **5a**, the gold(III) atom has distorted square-planar coordination and is bonded to a chloride ligand, two nitrogen atoms from pyridyl groups, and one amido nitrogen atom from the BPMA–H ligand (Figure 4). The bond from

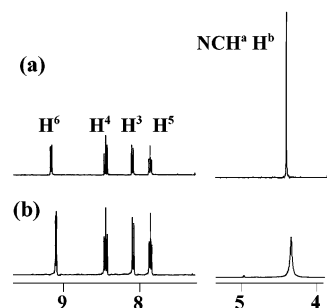


**Figure 3.** <sup>1</sup>H NMR spectra (400 MHz) of complex **5a** in acetone-*d*<sub>6</sub> at (a) 20 and (b) –60 °C.

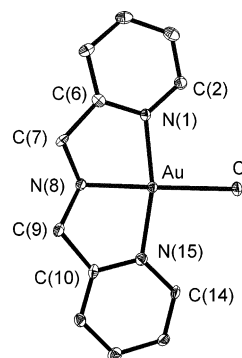


**Figure 4.** View of the structure of complex **5a**.

gold(III) to the amido nitrogen is slightly shorter than those to the pyridyl nitrogen atoms (Table 1). The main distortion from square-planar coordination is associated with the formation of the five-membered chelate rings, with angle N(1)AuN(15) = 165.4(2)°. The amido nitrogen atom has trigonal-pyramidal stereochemistry [sum of angles at N(8) = 330(1)°; Table 1], and the two methylene carbon atoms are displaced to the same side of the square plane [displacements of C(7) and C(9) = 0.60 and 0.55 Å; Table 2], such that the two pyridyl groups are close to coplanarity (Table 2). The structural data indicate that there is limited  $\pi$ -bonding between gold(III) and the amido nitrogen atom and that there is a stereochemically active lone pair of electrons on the nitrogen atom (Table 1 and theoretical studies below). The molecular structures of **5a–5c** are similar, as can be seen by comparison of the structural and conformational parameters in Tables 1 and 2.

The cations in complex **5b** pack in columns as shown in Figure 5. The closest Au $\cdots$ Au separations are Au $\cdots$ AuB = 3.54 Å and Au $\cdots$ AuA = 3.73 Å. The shorter of these distances is in the range expected for attractions between d<sup>8</sup>–d<sup>8</sup> complexes.<sup>13,14</sup> Such interactions are rare for gold(III), but they have been observed previously in a few bridged digold(III) compounds.<sup>13,14</sup> The antiparallel orientation of the square-planar gold(III) complexes (Au and AuB in Figure

(13) Vicente, J.; Chicote, M.-T.; Saura-Llamas, I.; Jones, P. G.; Meyer-Basle, K.; Erdbrugger, C. F. *Organometallics* **1988**, 7, 997.

(14) (a) Mendizabal, F.; Pykkö, P. *Phys. Chem. Chem. Phys.* **2004**, 6, 900. (b) Canales, S.; Crespo, O.; Gimeno, M. C.; Jones, P. G.; Laguna, A.; Mendizabal, F. *Organometallics* **2001**, 20, 4812. (c) Pykkö, P. *Angew. Chem., Int. Ed.* **2004**, 43, 4412. (d) Mendizabal, F.; Zapata-Torres, G.; Olea-Azar, C. *Chem. Phys. Lett.* **2003**, 382, 92. (e) Bennett, M. A.; Hockless, D. C. R.; Rae, A. D.; Welling, L. L.; Willis, A. C. *Organometallics* **2001**, 20, 79.

**Table 1.** Selected Bond Distances and Angles for Complexes **5a–5c** and **6** and DFT-Calculated Values for  $[\text{AuCl}(\text{BPMA}-\text{H})]^+$  (**5<sub>calc</sub>**) and  $[\text{AuCl}(\text{BPMA})]^{2+}$  (**6<sub>calc</sub>**)

	<b>5a</b>	<b>5b</b>	<b>5c</b>	<b>6</b>	<b>5<sub>calc</sub></b>	<b>6<sub>calc</sub></b>
Au–N(1)	2.014(6)	2.03(1)	2.025(8)	2.006(8)	2.05	2.05
Au–N(8)	1.994(5)	1.96(1)	1.974(9)	2.008(7)	2.03	2.09
Au–N(15)	2.023(6)	2.00(1)	2.008(9)	2.006(8)	2.05	2.05
Au–Cl	2.341(2)	2.335(3)	2.342(3)	2.265(3)	2.39	2.33
N(1)–Au–N(15)	165.4(2)	164.8(4)	164.5(4)	166.5(3)	163	165
N(8)–Au–Cl	176.8(2)	172.8(3)	175.9(2)	179.1(3)	174	179
C(7)–N(8)–C(9)	113.4(6)	113(1)	113.3(8)	122.3(9)	115	119
C(7)–N(8)–Au(1)	107.7(4)	110(1)	107.4(6)	109.5(6)	108	106
C(9)–N(8)–Au(1)	108.6(4)	108(1)	110.2(6)	109.8(6)	108	106
$\Sigma\text{N}(8)^a$	330	331	331	342	331	331

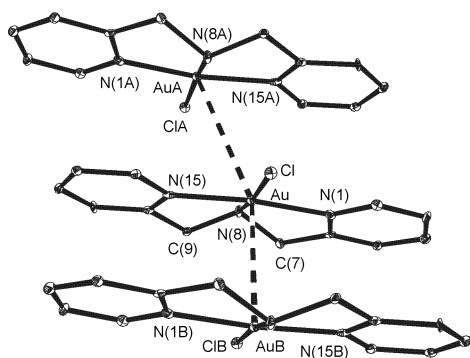
<sup>a</sup>  $\Sigma\text{N}(8)$  = sum of bond angles at the amido (**5a–5c**) or amine (**6**) nitrogen atom N(8).

**Table 2.** Conformational Parameters for Complexes **5a–5c** and **6**

	<b>5a</b>	<b>5b</b>	<b>5c</b>	<b>6</b>
AuN(8)C(7)C(6)	36	32	40	27
AuN(8)C(9)C(10)	32	32	29	30
N(8)C(7)C(6)N(1)	26	22	30	21
N(8)C(9)C(10)N(15)	23	24	22	24
$\delta\text{C}(7)^a$	0.60	0.47	0.62	0.45
$\delta\text{C}(9)^a$	0.55	0.45	0.47	0.50
$\omega\text{AuN}(1)^b$	13	9	13	9
$\omega\text{AuN}(15)^b$	11	7	8	10
$\omega\text{N}(1)\text{N}(15)^c$	2	2	7	6

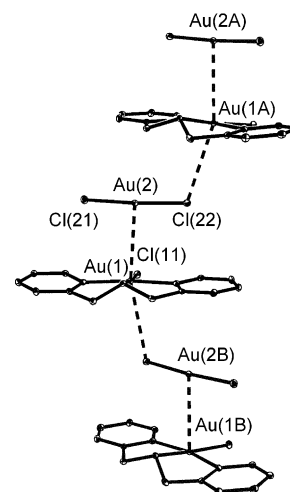
<sup>a</sup>  $\delta\text{C}$  = displacement ( $\text{\AA}$ ) of the carbon atom from the  $\text{AuN}_3\text{Cl}$  plane.

<sup>b</sup>  $\omega\text{AuN}$  = angle between the plane of the pyridyl group (containing N1 or N15) and the plane of the  $\text{AuN}_3\text{Cl}$  atoms. <sup>c</sup>  $\omega\text{N}(1)\text{N}(15)$  = angle between the planes of the two pyridyl groups.

**Figure 5.** Packing of the  $[\text{AuCl}(\text{BPMA}-\text{H})]^+$  ions in complex **5b**. Symmetry operators: A,  $-x + 1, -y + 2, -z + 2$ ; B,  $-x + 2, -y + 2, -z + 2$ .

**5**) is expected to minimize electrostatic repulsions between the chloride ligands and also allows  $\pi$ – $\pi$  stacking interactions between the pyridyl groups.<sup>14</sup>

The structure of complex **5c** is shown in Figure 6. The complex packs in columns with alternating gold(III) complex cations and gold(I) complex anions. There is a short aurophilic bond with  $\text{Au}(1) \cdots \text{Au}(2) = 3.34 \text{ \AA}$ . However, on the other side of the gold(III) center, the shortest contact is to a chloride ligand, with  $\text{Au}(1) \cdots \text{Cl}(22\text{B}) = 3.49 \text{ \AA}$  (Figure 6). There are few examples of  $\text{Au}(\text{I}) \cdots \text{Au}(\text{III})$  aurophilic bonds<sup>14</sup> or of gold(I) bound in an analogous way to other square-planar  $d^8$  metal ions.<sup>14–16</sup> Theoretical studies have indicated bonding energies for  $\text{Au}(\text{I}) \cdots \text{Au}(\text{III})$  secondary bonds that are close to those for the well-established

**Figure 6.** Structure of complex **5c**. Intermolecular distances:  $\text{Au}(1) \cdots \text{Au}(2) = 3.339 \text{ \AA}$ ,  $\text{Cl}(22) \cdots \text{Au}(1\text{A}) = 3.49 \text{ \AA}$ . Symmetry operators: A,  $1/2 + x, 1/2 - y, -1/2 + z$ ; B,  $-1/2 + x, 1/2 - y, 1/2 + z$ .

$\text{Au}(\text{I}) \cdots \text{Au}(\text{I})$  aurophilic bonds.<sup>14,17</sup> The dichloroaurate ion is oriented roughly parallel to the  $(\text{py})\text{N}-\text{Au}-\text{N}(\text{py})$  axis of the  $[\text{AuCl}(\text{BPMA}-\text{H})]^+$  ion in complex **5c**. This is the orientation that is expected on the basis of electrostatic factors. In the alternative orientation with the dichloroaurate ion oriented roughly parallel to the  $(\text{amido})\text{N}-\text{Au}-\text{Cl}$  axis of the  $[\text{AuCl}(\text{BPMA}-\text{H})]^+$  ion, there would be unfavorable electrostatic repulsions between the negatively charged ligands on gold(I) and gold(III).<sup>14</sup> The aurophilic bonds themselves arise from nondirectional dispersion forces and, therefore, do not control the preferred conformation.<sup>14</sup> We note that, if electrostatic forces alone were present, the orientation with the chloride ligands of the  $[\text{AuCl}_2]^-$  ion interacting with the cationic gold(III) center on both sides would be favored.

**Amido–Amine Equilibrium.** The amido complex **5a** reacted with excess triflic acid by protonation of the amido nitrogen atom to give the corresponding amine complex, isolated as the triflate salt  $[\text{AuCl}(\text{BPMA})](\text{OTf})_2$  (**6**; Scheme 4). The product has limited thermal stability in acid solution, and decomposition is accompanied by a color change from

(15) For a different type of gold(I)–gold(III) bond, see: Uson, R.; Laguna, A.; Laguna, M.; Torton, M. T.; Jones, P. G. *J. Chem. Soc., Chem. Commun.* **1988**, 740.

(16) (a) Singh, A.; Sharp, P. R. *J. Chem. Soc., Dalton Trans.* **2005**, 2080. (b) Crespo, O.; Laguna, A.; Fernandez, E. J.; Lopez-de-Luzuriaga, J. M.; Jones, P. G.; Teichert, M.; Monge, M.; Pyykko, P.; Runeberg, N.; Schutz, M.; Werner, H.-J. *Inorg. Chem.* **2000**, 39, 4786. (17) (a) Schneider, D.; Schuster, O.; Schmidbaur, H. *Organometallics* **2005**, 24, 3547. (b) Fackler, J. P., Jr. *Inorg. Chem.* **2002**, 41, 6959.



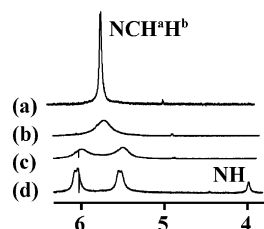
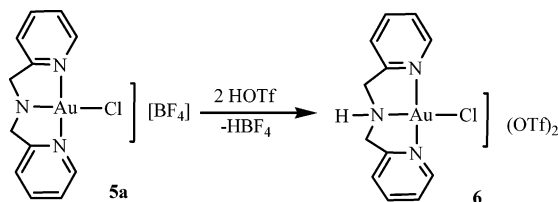


**Figure 7.**  $^1\text{H}$  NMR spectra (400 MHz, acetone- $d_6$ ) of complex **6** in the region of the  $\text{NCH}_2$  and  $\text{NH}$  resonances at temperatures of (a) 20, (b)  $-20$ , (c)  $-60$ , and (d)  $-90$   $^\circ\text{C}$ . The low intensity of the  $\text{NH}$  resonance occurs as a result of  $\text{H-D}$  exchange with solvent.

**Scheme 4**



pale yellow to black. The pure product **6** decomposes quickly in acetone, but is more stable in methanol solution. The  $\text{pK}_\text{a}$  value for **6**, obtained as described for diethylenetriamine derivatives,<sup>4</sup> is estimated at 3.5. For comparison, the  $\text{pK}_\text{a}$  values of  $[\text{AuCl}(\text{dien})]^{2+}$  and  $[\text{AuCl}(\text{Et}_4\text{dien})]^{2+}$  are estimated to be 4.0 and 2.2, respectively, and the spectroscopic changes accompanying protonation or deprotonation are similar in each case.<sup>4</sup>

In the  $^1\text{H}$  NMR spectrum in acetone- $d_6$  solution at room temperature, the  $\text{NCH}_2$  protons of complex **6** appeared as a single resonance at  $\delta = 5.66$ , considerably shifted from the value for **5a** of  $\delta = 4.44$ , consistent with transfer of some positive charge to the  $\text{CH}_2$  protons upon protonation of **5a**. There were smaller increases in the chemical shifts of the pyridyl protons in **6** compared to that of **5a** (see the Experimental Section). At lower temperatures, the  $\text{NCH}_2$  resonance gradually became broader and finally split into two peaks (Figure 7). No resonance for the  $\text{NH}$  proton was resolved except at very low temperature (Figure 7), and the intensity was low as a result of  $\text{H-D}$  exchange with the solvent. The changes in the  $^1\text{H}$  NMR spectra as a function of temperature are interpreted in terms of overall inversion at the amine nitrogen atom, which leads to effective equivalence of the  $\text{CH}_2\text{H}^b$  protons of each methylene group. The mechanism is likely to involve reversible deprotonation of the amine group, with inversion at the nitrogen of the amido derivative, as shown in Scheme 5. The inversion at nitrogen is slowed by the addition of free triflic acid. The protonation of **5a** in acetone- $d_6$  with  $\text{H}[\text{PF}_6]$  gives NMR spectra very similar to those reported for **6**, but it has not been possible to isolate this product in pure form. It is likely that the hydrogen bonding of the  $\text{NH}$  proton of **6** with triflate is less important in solution than in the solid state (see below).<sup>18</sup>

The structure of complex **6** is shown in Figure 8, and its structural parameters are included in Tables 1 and 2. The overall structure is similar to those of **5a–5c** (Tables 1 and 2), but there are subtle differences. For example, the  $\text{Au-N}(8)$  bond in **6** [ $2.008(7)$  Å] is longer than that in **5a** [ $1.994$ –

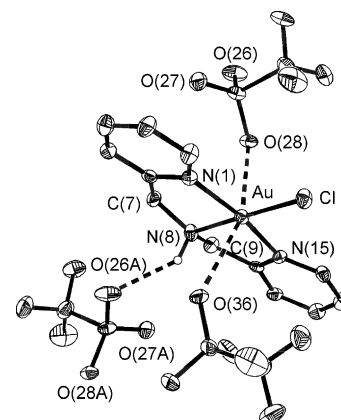
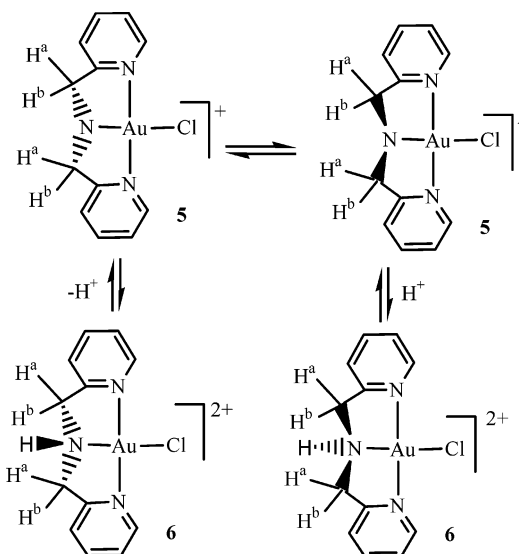


**Figure 8.** View of the structure of the complex  $[\text{AuCl}(\text{BMPA})](\text{OTf})_2$ , **6**. Two triflate ions involved in  $\text{NH}\cdots\text{O}-\text{S}-\text{O}\cdots\text{Au}$  bridging are shown.

**Scheme 5**



(5) Å], whereas the  $\text{Au-Cl}$  bond in **6** [ $2.265(3)$  Å] is shorter than in **5a** [ $2.341(2)$  Å]. Hence, protonation of the amido nitrogen weakens the  $\text{Au-N}$  bond because the amine nitrogen is a weaker  $\sigma$ -donor than the amido nitrogen. Because the amido nitrogen in **5a** is a stronger  $\sigma$ -donor than the amine nitrogen donor in **6**, it has a stronger trans influence than the amine nitrogen donor, and so, the  $\text{Au-Cl}$  bond is longer in **5a** than in **6**. It is interesting that protonation of the nitrogen atom leads to a less pyramidal stereochemistry at  $\text{N}(8)$  in **6** than in **5a**. Thus, the sum of the bond angles at  $\text{N}(8)$  (Table 1) is greater in **6** ( $342^\circ$ ) than in **5a** ( $330^\circ$ ), as expected if there were little  $\text{Au-N}(8)$   $\pi$ -bonding in the amido complexes.

In complex **6**, both triflate ions are weakly coordinated to gold(III) with  $\text{Au}\cdots\text{O}(36) = 2.79$  Å and  $\text{Au}\cdots\text{O}(28) = 2.84$  Å. In addition, there is a hydrogen bond between the  $\text{NH}$  group of **6** and one of the oxygen atoms of a triflate anion of a neighboring formula unit [ $\text{N}(8)\cdots\text{O}(26\text{A}) = 2.98(1)$  Å]. The bridging of the triflate ion  $\text{N}(8)\text{H}\cdots\text{O}(26\text{A})-\text{S}-\text{O}(28\text{A})\cdots\text{Au}(\text{A})$  leads to formation of a supramolecular polymer.

(18) (a) Romeo, R.; Minniti, D.; Alibrandi, G.; de Cola, L.; Tobe, M. L. *Inorg. Chem.* **1986**, 25, 1944. (b) Romeo, R.; Nastasi, N.; Scolaru, M.; Plutino, M. R.; Albinati, A.; Macchioni, A. *Inorg. Chem.* **1998**, 37, 5460.

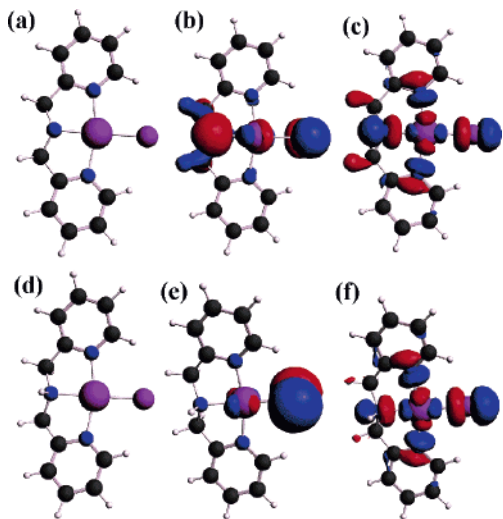


**Figure 9.** (a,d) Calculated structures, (b,e) HOMOs, and (c,f) LUMO for complexes (a–c) **5** and (d–f) **6**.

**Theoretical Studies.** To gain further insight into the structural features of complexes **5** and **6**, calculations were carried out on the cations  $[\text{AuCl}(\text{BPMA-H})]^+$  and  $[\text{AuCl}(\text{BPMA})]^{2+}$  using density functional theory (DFT), with a relativistic potential for gold.<sup>19</sup> Data are reported in Table 1 and in Figure 9. Table 1 shows that the DFT calculations give reasonable values for the bond distances and also accurately predict the trigonal-pyramidal stereochemistry of the amido nitrogen atom in **5** (calculated sum of bond angles at N = 331°). The calculation also predicts the longer Au–Cl and shorter Au–N(amide) distances in **5** compared to **6** (Table 1).

In complex **5**, the HOMO (Figure 9b) has mostly the character of the amido nitrogen lone pair, with smaller components from gold ( $5d_{x^2-y^2}$ ,  $5d_{xy}$ ,  $5d_{z^2}$ ) and chlorine ( $3p_z$ ), while the LUMO (Figure 9c) is the  $\sigma^*(\text{Au } 5d_{x^2-y^2})$  molecular orbital. The gold  $6p_z$  orbital is too high in energy to play a significant part in the bonding, and the lack of  $\pi$ -bonding with this gold  $6p_z$  orbital accounts for the pyramidal stereochemistry of the amido nitrogen atom in **5**. Protonation of the amido nitrogen lone pair in **5** leads to stabilization of the  $\sigma(\text{NH})$  orbital in **6**, and the HOMO in **6** (Figure 9e) has mostly chlorine  $3p_z$  character. The character of the LUMO in **6** (Figure 9f) is similar to that in **5** (Figure 9c).

For the trans N–Au–Cl atoms, the Hirschfeld analysis of the atomic charges is useful.<sup>19</sup> These charges are N, –0.16e; Au, 0.44e; and Cl, –0.16e in **5** and N, –0.03e; Au, 0.50e; and Cl, –0.06e in **6**. The charge on the NH proton in **6** is calculated to be 0.48e. Thus, upon protonation of **5**, a charge of 0.52e is transferred from **5** to the proton, and this is contributed by the atoms of the trans N–Au–Cl unit (0.29e, consisting of 0.13e from N, 0.06e from Au, and 0.10e from Cl) and by the atoms of the pyridylmethyl groups (0.23e). Of course, this transfer of charge is fully consistent with the concept of a trans influence, in which the stronger

amide donor in **5** compared to the amine donor in **6** leads to weakening and polarization of the trans Au–Cl bond in **5**.

## Conclusions

The neutral ligands BBPMA and BPMA can coordinate to gold(III) to give the cationic complexes  $[\text{AuCl}(\text{BBPMA})]^{2+}$  (**3**; Scheme 2) and  $[\text{AuCl}(\text{BPMA})]^{2+}$  (**6**; Scheme 4). The gold(III) center is strongly polarizing, and the effect is exhibited by the activation of a C–N bond of complex **3** (Scheme 2) or by the easy deprotonation of complex **6** to give the corresponding amido complex  $[\text{AuCl}(\text{BPMA-H})]^+$  (**5**; Schemes 3 and 4). The much greater polarizing power of gold(III) compared to, for example, platinum(II) is seen in the differences in pKa values for  $[\text{Pt}(\text{DMSO})(\text{dien})]^{2+}$  (11.9),<sup>18</sup>  $[\text{AuCl}(\text{dien})]^{2+}$  (4.0),<sup>4a</sup>  $[\text{Pt}(\text{OH})(\text{BPMA})]^+$  (11.5),<sup>11a</sup> and  $[\text{AuCl}(\text{BPMA})]^{2+}$  (3.5). This difference is not purely an oxidation-state phenomenon, as BPMA complexes of molybdenum(V) are not spontaneously deprotonated.<sup>20</sup> The difference between gold(III) and platinum(II) is important in coordination chemistry, and especially in aqueous bioinorganic chemistry, because under normal conditions, the BPMA complexes of platinum(II) and gold(III) exist in the amine (BPMA) and amido (BPMA–H) forms, respectively.<sup>10–13,18,21</sup> The ability of gold(III) to act as a strong  $\sigma$ -electrophile, with intermediate hard–soft character, is considered to be a key property in the bond-activation reactions involved in catalytic chemistry.<sup>1</sup>

The stronger trans influence of the amido group in **5** compared to the amine group in **6** on the trans Au–Cl bond is evident from the structure determinations and also from the DFT calculations (Table 1). Previous work has shown that the trans effect, measured by the rate of ligand substitution, tends to be higher for the amido ligand with neutral nucleophiles and higher for the amine group with anionic nucleophiles.<sup>4,18</sup> The present work suggests that the actual ligand-substitution step should be faster for the trans amide but that the more favorable pre-equilibrium of anionic reagents  $\text{X}^-$  with the dicationic amine complex  $\{[\text{AuCl}(\text{BPMA})]^{2+} \cdots \text{X}^-\}$  in the case of **6** compared to the monocationic amido complex  $\{[\text{AuCl}(\text{BPMA-H})]^+ \cdots \text{X}^-\}$  in the case of **5** can mask this effect.

The nearly planar structure of  $[\text{AuCl}(\text{BPMA-H})]^+$  allows easy axial approach to the gold(III) center, and there is a competition between electrostatic attraction to negatively charged anions or dipoles and the formation of aurophilic bonds. Unusual examples of  $\text{Au(III)} \cdots \text{Au(III)}$  and  $\text{Au(III)} \cdots \text{Au(I)}$  aurophilic bonds are identified, in which the orientation of the two gold units is mostly controlled by electrostatic interactions between the supporting ligands on each gold center.<sup>14</sup>

## Experimental Section

NMR spectra were recorded using a Varian Mercury or Inova 400 NMR spectrometer. The ligands BPMA and BBPMA were prepared according to the literature methods.<sup>22</sup>

(19) (a) Baerends, E. J. et al. *ADF2006.01*; Vrije Universiteit: Amsterdam, The Netherlands, 2006; available at <http://www.scm.com>. (b) Becke, A. D. *J. Chem. Phys.* **1993**, 98, 5648. (c) Hirschfeld, F. L. *Theor. Chim. Acta* **1977**, 44, 129.

(20) van Staveren, D. R.; Bothe, E.; Weyhermüller, T.; Metzler-Nolte, N. *Eur. J. Inorg. Chem.* **2002**, 1518.

(21) Gibson, D. H.; Wu, J. G.; Mashuta, M. S. *Inorg. Chim. Acta* **2006**, 359, 309.

**Table 3.** Crystal Data for Compounds **2a**, **2b**, and **4**

	<b>2a</b>	<b>2b</b>	<b>4</b>
formula	C <sub>19</sub> H <sub>21</sub> AuCl <sub>5</sub> N <sub>3</sub>	C <sub>19</sub> H <sub>21</sub> AuCl <sub>3</sub> N <sub>3</sub>	C <sub>13</sub> H <sub>16</sub> Cl <sub>2</sub> N <sub>2</sub>
fw	665.6	594.7	271.2
<i>T</i> (K)	150(2)	150(2)	299(2)
$\lambda$ (Å)	0.71073	0.71073	0.71073
cryst syst	orthorhombic	orthorhombic	triclinic
space group	<i>Pnma</i>	<i>Pbca</i>	<i>P</i> $\bar{1}$
cell dimens			
<i>a</i> (Å)	13.5338(3)	11.7116(3)	5.0844(4)
<i>b</i> (Å)	7.7333(2)	14.5205(4)	11.8297(7)
<i>c</i> (Å)	21.7974(6)	23.9645(6)	12.038(1)
$\alpha$ (deg)	90	90	93.929(5)
$\beta$ (deg)	90	90	98.807(3)
$\gamma$ (deg)	90	90	94.546(4)
<i>V</i> (Å <sup>3</sup> )	2281.3(1)	4075.4(2)	710.9(1)
<i>Z</i>	4	8	2
<i>d</i> (calcd) (Mg m <sup>−3</sup> )	1.938	1.939	1.267
$\mu$ (mm <sup>−1</sup> )	7.045	7.621	0.437
<i>F</i> (000)	1280	2288	284
abs corr	integration	integration	integration
data/constr/params	3566/0/196	4665/0/236	2470/0/172
GOF	1.076	1.021	1.054
R1 [ <i>I</i> > 2 $\sigma$ ( <i>I</i> )]	0.042	0.036	0.062
wR2 [ <i>I</i> > 2 $\sigma$ ( <i>I</i> )]	0.091	0.096	0.168

**[(BBPMA)H<sub>2</sub>]Cl[AuCl<sub>4</sub>], 2a.** To a solution of HAuCl<sub>4</sub>·3H<sub>2</sub>O (0.394 g, 1.00 mmol) in acetone (20 mL) was added a solution of BBPMA (0.290 g, 1.00 mmol) in acetone (5 mL). The mixture was stirred for 5 h at room temperature; then, the solution was filtered, the volume of the filtrate was reduced to 5 mL under vacuum, and pentane (20 mL) was added to precipitate the product as a pale brown solid. The product was filtered, washed with ether and pentane, and recrystallized from acetone/pentane. Yield: 85%. Mp: 117 °C (decomp). Anal. Calcd for C<sub>19</sub>H<sub>21</sub>AuCl<sub>5</sub>N<sub>3</sub>: C, 34.28; H, 3.18; N, 6.31%. Found: C, 33.97; H, 3.06; N, 6.22%. NMR in acetone-*d*<sub>6</sub>:  $\delta$ (<sup>1</sup>H) = 8.93 (d, 2H, py-H<sup>6</sup>), 8.59 (m, 2H, py-H<sup>4</sup>), 8.06–8.11 (m, 4H, py-H<sup>3</sup>, H<sup>5</sup>), 7.43 (d, 2H, ph-H<sup>2</sup>H<sup>6</sup>), 7.08–7.18 (m, 3H, Ph–H<sup>3</sup>H<sup>4</sup>H<sup>5</sup>), 4.33 (s, 4H, N–CH<sub>2</sub>–py), 3.99 (s, 2H, N–CH<sub>2</sub>–Ph).

**[(BBPMA)H<sub>2</sub>]Cl[AuCl<sub>2</sub>], 2b.** This compound was prepared similarly to **2a**, but the reaction solution was heated under reflux for 3 h. Yield: 53%. Anal. Calcd for C<sub>19</sub>H<sub>21</sub>AuCl<sub>3</sub>N<sub>3</sub>: C, 38.37;

H, 3.56; N, 7.07%. Found: C, 38.01; H, 3.34; N, 6.96%. The NMR data were very similar to the data for **2a**. Crystals were grown from acetone/ether.

**[AuCl(BBPMA)]Cl<sub>2</sub>, 3.** To a stirred solution of NaAuCl<sub>4</sub> (0.338 g, 1.00 mmol) in H<sub>2</sub>O (20 mL) was added a solution of BBPMA (0.267 g, 1.00 mmol). The mixture was stirred for 4 h to give the product as a brown solid precipitate, which was separated by filtration; washed with H<sub>2</sub>O, ethanol, Et<sub>2</sub>O, and pentane; and dried under vacuum. Yield: 57%. Mp: 138–141 °C (decomp). Anal. Calcd for C<sub>19</sub>H<sub>19</sub>AuCl<sub>3</sub>N<sub>3</sub>: C, 38.50; H, 3.23; N, 7.09%. Found: C, 38.28; H, 3.03; N, 6.98%. NMR in nitromethane-*d*<sub>3</sub>:  $\delta$ (<sup>1</sup>H) = 8.73 (d, 2H, py-H<sup>6</sup>), 8.21 (m, 2H, py-H<sup>4</sup>), 7.72 (d, 2H, py-H<sup>3</sup>), 7.60 (m, 2H–py-H<sup>5</sup>), 7.48 (d, 2H, Ph–H<sup>2</sup>H<sup>6</sup>), 7.10–7.15 (m, 3H·Ph–H<sup>3</sup>H<sup>4</sup>H<sup>5</sup>), 5.75 (d, 2H, N–CH<sup>a</sup>H<sup>b</sup>–py), 5.19 (d, 2H, N–CH<sup>a</sup>H<sup>b</sup>–py), 4.86 (s, 2H, N–CH<sub>2</sub>–Ph).

**[PhCH<sub>2</sub>NH<sub>2</sub>CH<sub>2</sub>–2–C<sub>5</sub>H<sub>4</sub>NH]Cl<sub>2</sub>, 4.** To a solution of NaAuCl<sub>4</sub> (0.415 g, 1.18 mmol) in distilled water (30 mL) was added BBPMA (0.342 g, 1.18 mmol). The mixture was stirred for 12 h at 80 °C, cooled to room temperature, and filtered to remove insoluble material, and the solvent from the filtrate was evaporated under vacuum. The solid product was recrystallized from MeOH/Et<sub>2</sub>O. Yield: 35%. Mp: 125–129 °C (decomp). Anal. Calcd for C<sub>13</sub>H<sub>16</sub>Cl<sub>2</sub>N<sub>2</sub>: C, 57.58; H, 5.95; N, 10.33%. Found: C, 57.51; H, 5.83; N, 9.97%. NMR in CD<sub>3</sub>OD:  $\delta$ (<sup>1</sup>H) = 8.87 (d, 1H, py-H<sup>6</sup>), 8.44 (m, 1H, py-H<sup>4</sup>), 8.06 (d, 1H, py-H<sup>3</sup>), 7.92 (m, 1H, py-H<sup>5</sup>), 7.60 (m, 2H, Ph–H<sup>2</sup>H<sup>6</sup>), 7.45–7.50 (m, 3H, Ph–H<sup>3</sup>H<sup>4</sup>H<sup>5</sup>), 4.65 (s, 2H, N–CH<sub>2</sub>–py), 4.43 (s, 2H, N–CH<sub>2</sub>–Ph).

**[AuCl(BPMA–H)]PF<sub>6</sub>, 5b.** To a solution of NaAuCl<sub>4</sub> (0.873 g, 2.22 mmol) in H<sub>2</sub>O (30 mL) was added NaHCO<sub>3</sub> (0.306 g, 2.22 mmol) and KPF<sub>6</sub> (0.815 g, 4.43 mmol). To this solution was added dropwise a solution of BPMA (0.455 g, 2.22 mmol) in MeOH (5 mL). The product precipitated as a red solid, which was separated by filtration; washed with H<sub>2</sub>O (2 × 30 mL), EtOH (30 mL), and ether (3 × 30 mL); and recrystallized from acetone/ether. Yield: 1.19 g, 90%. Mp: 112 °C (decomp). Anal. Calcd for C<sub>12</sub>H<sub>12</sub>–AuClF<sub>6</sub>N<sub>3</sub>P: C, 25.04; H, 2.10; N, 7.30%. Found: C, 24.69; H, 2.02; N, 7.18%. NMR in acetone-*d*<sub>6</sub>:  $\delta$ (<sup>1</sup>H) = 9.15 (d, 2H, py-H<sup>6</sup>), 8.46 (m, 2H, py-H<sup>4</sup>), 8.12 (d, 2H, py-H<sup>3</sup>), 7.91 (t, 2H, py-H<sup>5</sup>), 4.44 (s, 4H, CH<sub>2</sub>).

**[AuCl(BPMA–H)]BF<sub>4</sub>, 5a.** This compound was prepared in a similar way except that NaBF<sub>4</sub> was used in place of KPF<sub>6</sub>. Yield:

**Table 4.** Crystal Data for Compounds **5a–5c** and **6·Me<sub>2</sub>CO**

	<b>5a</b>	<b>5b</b>	<b>5c</b>	<b>6·Me<sub>2</sub>CO</b>
formula	C <sub>12</sub> H <sub>12</sub> AuBClF <sub>4</sub> N <sub>3</sub>	C <sub>12</sub> H <sub>12</sub> AuClF <sub>6</sub> N <sub>3</sub> P	C <sub>12</sub> H <sub>12</sub> Au <sub>2</sub> Cl <sub>3</sub> N <sub>3</sub>	C <sub>17</sub> H <sub>19</sub> AuClF <sub>6</sub> N <sub>3</sub> O <sub>7</sub> S <sub>2</sub>
fw	517.47	575.63	698.53	787.89
<i>T</i> (K)	150(2)	150(2)	296(2)	150(2)
$\lambda$ (Å)	0.71073	0.71073	0.71073	0.71073
cryst syst	monoclinic	triclinic	monoclinic	monoclinic
space group	<i>P2<sub>1</sub>/c</i>	<i>P</i> $\bar{1}$	<i>P2<sub>1</sub>/n</i>	<i>P2<sub>1</sub>/n</i>
cell dimens				
<i>a</i> (Å)	14.3491(8)	7.1133(8)	7.4839(3)	8.4086(4)
<i>b</i> (Å)	7.6628(3)	9.2734(1)	19.8209(7)	13.8090(7)
<i>c</i> (Å)	14.2562(8)	13.218(2)	10.7631(4)	22.193(1)
$\alpha$ (deg)	90	108.123(5)	90	90
$\beta$ (deg)	112.434(2)	97.509(7)	95.441(2)	97.336(3)
$\gamma$ (deg)	90	102.762(7)	90	90
<i>V</i> (Å <sup>3</sup> )	1448.9(1)	789.3(2)	710.9(1)	2555.8(2)
<i>Z</i>	4	2	4	4
<i>d</i> (calcd) (Mg m <sup>−3</sup> )	2.372	2.422	2.919	2.048
$\mu$ (mm <sup>−1</sup> )	10.379	9.655	18.935	6.111
<i>F</i> (000)	968	540	1256	1520
abs corr	integration	integration	integration	integration
data/constr/params	2557/4/200	2780/0/217	2793/0/182	4501/0/335
GOF	0.983	1.044	0.964	1.048
R1 [ <i>I</i> > 2 $\sigma$ ( <i>I</i> )]	0.035	0.051	0.038	0.054
wR2 [ <i>I</i> > 2 $\sigma$ ( <i>I</i> )]	0.056	0.105	0.087	0.091

88%. Mp: 102–103 °C. Anal. Calcd for  $C_{12}H_{12}AuBClF_4N_3$ : C, 27.85; H, 2.34; N, 8.12%. Found: C, 27.56; H, 2.09; N, 7.86%. NMR in acetone- $d_6$  similar to **5b**.

**[AuCl(BPMA–H)][AuCl<sub>2</sub>], 5c.** This compound was prepared similarly to **5b** but with no KPF<sub>6</sub> added and with a reaction time of 4 h. A red powder was obtained and was recrystallized from acetone/pentane. Yield: 91% (based on gold). Mp: 114 °C (decomp). Anal. Calcd for  $C_{12}H_{12}Au_2Cl_3N_3$ : C, 20.63; H, 1.73; N, 6.02%. Found: C, 21.02; H, 1.95; N, 6.21%. NMR in DMSO- $d_6$ :  $\delta(^1H)$  = 8.97 (d, 2H, py-H<sup>6</sup>), 8.35 (t, 2H, py-H<sup>4</sup>), 8.00 (d, 2H, py-H<sup>3</sup>), 7.78 (t, 2H, py-H<sup>5</sup>), 4.13 (s, 4H, CH<sub>2</sub>).

**[AuCl(BPMA)](OTf)<sub>2</sub>, 6.** To a red suspension of complex **5a** (0.183 g, 0.319 mmol) in acetone (10 mL) was added HOTf (0.056 mL, 0.64 mmol). The red color changed to pale yellow. The volume was reduced to ~3 mL under vacuum, and the precipitate was washed with ether (2 × 10 mL) and pentane (10 mL) and recrystallized from methanol/ether. Yield: 0.152 g, 72%. Mp: 163 °C (decomp). Anal. Calcd for  $C_{14}H_{13}AuClF_6N_3O_6S_2$ : C, 23.04; H, 1.80; N, 5.76%. Found: C, 23.23; H, 2.06; N, 5.90%. NMR in acetone- $d_6$ :  $\delta(^1H)$  = 9.14 (m, 2H, py-H<sup>6</sup>), 8.64 (m, 2H, py-H<sup>4</sup>), 8.20 (m, 2H, py-H<sup>3</sup>), 8.05 (m, 2H, py-H<sup>5</sup>), 5.56 (s, 4H, CH<sub>2</sub>).

(22) (a) Gruenwedel, D. W. *Inorg. Chem.* **1968**, 7, 495. (b) Dick, S.; Weiss, A. *Z. Naturforsch. B* **1997**, 52, 188.

**DFT Calculations.** Calculations were carried out using the Amsterdam density functional theory package ADF2006.01.<sup>19</sup> The hybrid functional BLYP was used, with a relativistic potential for gold.<sup>19</sup> Atomic charges were estimated using the Hirschfeld procedure.<sup>19</sup>

**X-ray Structure Determinations.** A crystal was mounted on a glass fiber. Data were collected using a Nonius Kappa-CCD diffractometer with COLLECT software. Unit cell parameters were calculated and refined from the full data set, and the absorption correction was made using the HKL2000 DENZO-SMN program. The refinement was carried out using the SHELXTL/PC 6.14 programs. Non-hydrogen atoms were refined anisotropically, and hydrogen-atom positions were included as riding on the respective carbon or nitrogen atom. Details are reported in Tables 3 and 4.

**Acknowledgment.** We thank the NSERC (Canada) for financial support. R.J.P. thanks the Government of Canada for a Canada Research Chair.

**Supporting Information Available:** X-ray data as electronic CIF files. Structure of the tetrachloroaurate salt **2a** (Figure S1) and crystallographic characterization of [PhCH<sub>2</sub>NH<sub>2</sub>CH<sub>2</sub>–2-C<sub>3</sub>H<sub>4</sub>NH]Cl<sub>2</sub>, **4** (Figure S2). This material is available free of charge via the Internet at <http://pubs.acs.org>.

IC061911Y